

Bcl-2–Enhanced Efficacy of Microtubule-Targeting Chemotherapy through Bim Overexpression: Implications for Cancer Treatment¹

Amandine Savry, Manon Carre, Raphael Berges, Amandine Rovini, Isabelle Pobel, Christine Chacon, Diane Braguer and Véronique Bourgairel-Rey

INSERM UMR911, Centre de Recherche en Oncologie Biologique et Oncopharmacologie, Aix-Marseille Université, Faculté de Pharmacie, Marseille Cedex, France

Abstract

Bcl-2 is commonly overexpressed in tumors, where it is often associated with unfavorable outcome. However, it has also been linked to a favorable sensitivity to microtubule-targeting agents (MTAs). We show that Bcl-2–overexpressing lung and breast cancer cells were more sensitive to both paclitaxel and vinorelbine. Bcl-2 overexpression also significantly potentiated *in vivo* efficacy of paclitaxel, in terms of tumor volume decrease and survival benefits, in models of nude mice bearing lung cancer xenografts. To further investigate this favorable effect of Bcl-2, a genomic approach was taken. It revealed that Bcl-2 overexpression induced up-regulation of the proapoptotic protein Bim in lung cancer cells and that, conversely, Bcl-2 silencing decreased Bim expression level. A gene regulation study implicated the transcription factor Forkhead box-containing protein, class O3a in Bim up-regulation. Lastly, we show that Bim was responsible for MTA-triggered lung cancer cell death through a dynamin-related protein 1–mediated mitochondrial fragmentation. The Bcl-2–governed Bim induction evidence offers for the first time an explanation for the favorable higher sensitivity to treatment shown by Bcl-2–overexpressing cells. We suggest that Bim could be a powerful predictive factor for tumor response to MTA chemotherapy. Our data also give new insight into some failures in the efficacy of therapies targeted against Bcl-2.

Neoplasia (2013) 15, 49–60

Introduction

Microtubule-targeting agents (MTAs) are known to inhibit cancer expansion through both antitumor and antiangiogenic properties. This therapeutic class is used to treat a broad range of solid tumors, including neuroblastoma and lung and breast cancers. It is well known that MTAs commonly disturb dynamics of the microtubule plus ends [1,2] and induce cell death through the mitochondrial apoptotic pathway [3,4]. Whether a cell survives or dies through apoptosis is determined by the relative levels of Bcl-2 family proteins. The antiapoptotic members, such as Bcl-2, secure mitochondrial integrity, whereas the proapoptotic members, such as Bim, facilitate the release of apoptogenic factors from the intermembrane space of mitochondria to cytosol [5]. In MTA-treated cells, the mitochondrial network undergoes very marked morphologic changes, from long tubular to short punctiform structures [3]. This fragmentation may contribute to mitochondrial injury and release of apoptogenic factors in the cytosol [6,7]. The dynamin-related protein 1 (Drp1) is crucial for fission [8,9], but growing evidence suggests that members of the Bcl-2 family may also be

involved in the regulation of the mitochondrial network organization [10,11].

Overexpression of Bcl-2 is commonly found in various types of cancer and is generally regarded as a biomarker of resistance to both radiotherapy and chemotherapy [12–14]. Accordingly, targeted therapies directed to Bcl-2, such as the Bcl-2 antisense oligodeoxynucleotide oblimersen, are now available for phase I to III clinical

Abbreviations: MTAs, microtubule-targeting agents; Drp1, dynamin-related protein 1; FoxO, Forkhead box-containing protein, class O

Address all correspondence to: Véronique Bourgairel-Rey, PhD, INSERM 911 CRO2, Faculté de Pharmacie, 27 boulevard Jean-Moulin, 13385 Marseille, France.

E-mail: veronique.rey.1@univ-amu.fr

¹This article refers to supplementary materials, which are designated by Figures W1 to W4 and are available online at www.neoplasia.com.

Received 4 July 2012; Revised 30 November 2012; Accepted 3 December 2012

Copyright © 2013 Neoplasia Press, Inc. All rights reserved 1522-8002/13/\$25.00
DOI 10.1593/neo.121074

trials [15]. However, these therapies have produced inconsistent results. For example, addition of oblimersen to carboplatin and etoposide did not improve clinical outcome measured in patients with small cell lung cancers [16]. Recent studies in breast and prostate cancers also concluded that the combination of oblimersen with docetaxel did not display any efficacy [17,18].

These discrepant results must be reanalyzed in the light of the controversial role of Bcl-2 in its resistance to anticancer drugs. Bcl-2 overexpression paradoxically enhanced *in vitro* sensitivity to docetaxel in non–small cell lung cancer [19] and to vinca alkaloids in breast cancer cells [20]. Consistent with this finding, low Bcl-2 expression levels were responsible for ovarian cancer cell resistance to paclitaxel and vinflunine, while reintroducing Bcl-2 restored cell sensitivity to treatment [21,22]. All these data support an equivocal role for Bcl-2 in the mechanism of action of MTAs. Conversely, there is no doubt about the involvement of Bim in MTA-induced apoptosis [23–25]. In healthy cells, Bim can bind to LC8 and is thereby sequestered to the microtubule-associated dynein motor complex [26]. In a previous study, we showed that MTA treatment caused Bim translocation to mitochondria to trigger neuroblastoma cell death. Studies that aim at deciphering the molecular mechanisms underlying Bim activation during MTA-induced apoptosis have revealed an important role for the transcriptional regulation of *bim* gene expression [27]. Bim transcription is mainly controlled by transcription factors of the Forkhead box-containing protein, class O (FoxO) family, which are inhibited by phosphorylation through phosphatidylinositol 3 kinase (PI3K), AKT, and serum and glucocorticoid-inducible kinases (SGKs) [28,29].

The aim of this study was to decipher the role of Bcl-2 in human cancer cell sensitivity or resistance to MTAs. The study design, using *bcl-2* gene transfer in tumor cell lines of different origins (lung, breast, and neuroblastoma), enables us to efficiently induce Bcl-2 overexpression, as observed in many patients [30–32]. This study may help us determine the best treatment for tumors that intrinsically overexpress Bcl-2 and so improve the outcome of these patients. First, we found that Bcl-2 overexpression selectively increased efficacy of paclitaxel and vinorelbine in lung and breast carcinoma cells. This finding was validated in nude mice bearing non–small cell lung cancer xenografts, where Bcl-2 overexpression potentiated *in vivo* paclitaxel efficacy. A genomic approach then showed that Bcl-2 overexpression was responsible for a significant increase in *bim* expression levels. We also found that Bim up-regulation was mediated by FoxO3a activation. Lastly, we show that Bim involvement in cell sensitivity to treatment relies on its ability to trigger the mitochondrial network fragmentation. We thus offer, for the first time, an explanation for the higher sensitivity to MTAs displayed by Bcl-2–overexpressing cancer cells. Taken together, our data strongly suggest that Bim could serve as a biomarker of choice in predicting treatment efficacy.

Materials and Methods

Cell Lines and Reagents

Human non–small cell lung carcinoma (A549), neuroblastoma (SHEP), and breast cancer (MCF-7) cells were purchased from ATCC (Molshheim, France). These three lines were transfected using Lipofectamine 2000 (Invitrogen, Carlsbad, CA) with an empty plasmid pUse (Upstate Biotechnology, Lake Placid, NY) for control cells (A549 pUse, SHEP pUse, or MCF-7 pUse) or with a plasmid containing human Bcl-2 cDNA (pUse Bcl-2 vector) kindly given by Ferlini [21]. Various stable transfectants were obtained after geneticin selection

(A549 Bcl-2, SHEP Bcl-2, and MCF-7 Bcl-2). All these lines were routinely cultured in RPMI supplemented with 10% FBS, 2% L-glutamine, and 1% penicillin and streptomycin, at 37°C with 5% CO₂. A stock solution of paclitaxel (Alexis, Lausen, Switzerland) was prepared in DMSO. Vinorelbine (Sigma, Steinheim, Germany) and doxorubicin (Dakota, Paris, France) were prepared in aqueous solutions.

Transfection Studies

siRNA Bim (signalSilence Bim siRNA I; Cell Signaling Technology, Beverly, MA) and siRNA Bcl-2 (HP validated siRNA 1027400, target sequence: AAC CGG GAG ATA GTG ATG AAG; Qiagen, Hilden, Germany) were transfected into A549 Bcl-2 cells. siRNA Bcl-2 was designed and validated to minimize the risk of off-target effects. siRNA Bim specifically inhibits Bim expression using RNA interference, a method whereby gene expression can be selectively silenced through the delivery of double-stranded RNA molecules into the cell. Non-targeting siRNA [Signalsilence control siRNA (Cell Signaling Technology) concerning Bim studies and AllStars Negative control siRNA (Qiagen) for Bcl-2 studies] was used as controls for non–sequence-specific effects of the transfected siRNA.

A549 wild-type cells (A549 w) were transfected with pcDNA₆ plasmid (pcDNA₆) or containing Bim_{EL} cDNA (pcDNA₆-Bim), kindly given by A. Vazquez [33]. These transfections were achieved using Lipofectamine 2000 (Invitrogen) according to the protocol supplied by the manufacturer.

Cytotoxicity Assay

Cells were seeded in 96-well plates to be treated for 48 or 72 hours with different agents: paclitaxel, vinorelbine, and doxorubicin. Doses of MTAs used to treat cells *in vitro* were in the range of plasma concentrations measured in the patient [34]. For A549 Bcl-2 cells, we tested the effect of mdivi-1, a small-molecule mitochondrial division inhibitor, at 1 μM with paclitaxel. Growth inhibition was measured using the 3-[4,5-dimethylthiazol-2-yl]-2,5-diphenyltetrazolium bromide (MTT) cell proliferation assay. This colorimetric assay allows the monitoring of cell survival *in vitro*. Each experiment included vehicle-treated cells (controls) that proliferate following an exponential model. For each dose of anticancer drug tested, results were expressed as percentage of survival cells, according to the following equation: $OD_{\text{treated cells}} \times 100 / OD_{\text{control cells}}$.

Animal Studies

All the experimental procedures and animal care complied with French official guidelines. Female BALB/c nude mice 6 to 8 weeks old were obtained from Charles River Laboratories (L'Arbresle, France). The animals were housed in a temperature- and humidity-controlled room with a 12-hour on-off light cycle and given free access to food and water.

A total of 5×10^6 A549 pUse or A549 Bcl-2 cells were inoculated subcutaneously into the right dorsal flanks of the nude mice. Experimental treatments were started when tumors reached about 50 mm³ in volume (day 0). Mice were then randomly divided into four groups: group 1 (A549 pUse-bearing mice, $n = 8$) and group 2 (A549 Bcl-2-bearing mice, $n = 7$) received vehicle solution (control groups); group 3 (A549 pUse-bearing mice, $n = 8$) and group 4 (A549 Bcl-2-bearing mice, $n = 7$) were injected with paclitaxel.

We selected an administration schedule of consecutive daily intravenous (*i.v.*) injections for 5 days for paclitaxel, based on effective similar schedules previously published [35,36]. Paclitaxel was given to tumor-bearing mice at a dose of 24 mg/kg/day, slightly less than

the maximum tolerable dose (28 mg/kg/day) in this schedule. Paclitaxel was dissolved at 24 mg/ml in ethanol/Cremophor EL (1:1) solution and stored at 4°C. This stock solution was diluted to 2.4 mg/ml with saline just before injection. Vehicle solution (ethanol/Cremophor EL/saline, 1:1:18) was given to control groups. The injections were administered through the tail vein after intraperitoneal anesthesia with xylazine (10 mg/kg)/ketamine (100 mg/kg). Tumor sizes were measured twice a week and were determined after caliper measurement of the largest and perpendicular diameters and the depth. Tumor volumes were calculated according to the following formula: length \times width \times depth \times 0.5236. Mice were allowed to live until their natural death or were sacrificed when their tumor volume exceeded 2000 mm³. Kaplan-Meier survival curves were plotted and statistically analyzed.

Mitochondrial Reducing Potential Analysis

To measure the mitochondrial reducing potential, we performed MTT assays after short-time treatments, as described previously [37]. Briefly, cells were incubated for 6 hours with culture medium containing both paclitaxel (growing concentrations) and MTT (0.5 mg/ml), and absorbance was measured at 550 nm.

Mitochondria Isolation and Western Blot Analysis

Whole-cell lysates and mitochondrial pellets were prepared as previously described [37,38]. Equal amounts of proteins were separated by sodium dodecyl sulfate–polyacrylamide gel electrophoresis and electrotransferred onto a nitrocellulose membrane. The membranes were then probed with antibodies directed against Bcl-2 (Dako, Glostrup, Denmark), Bim (BD Pharmingen, San Diego, CA), α -tubulin (Sigma), voltage-dependent anion channel (VDAC; Sigma), or caspase-9 (Abcam, Cambridge, United Kingdom). Blots were then labeled with peroxidase-conjugated secondary anti-mouse or anti-rabbit antibodies (Jackson ImmunoResearch, Baltimore, MD). Chemiluminescence imaging was performed with the Immobilon Western Chemiluminescent HRP substrate (Millipore, Billerica, MA) and the G-Box acquisition system (SynGene, Cambridge, United Kingdom). Signals were then quantified with the GeneTools analysis software, and mean values of three independent experiments are indicated in figures.

Flow Cytometry

After paclitaxel treatment for 24 hours, cells were fixed, permeabilized, and stained with propidium iodide as described previously [22]. Fluorescence was measured by flow cytometry (FACScan; BD Biosciences, San Jose, CA). The results obtained were analyzed by CellQuest Pro software (BD Biosciences).

Fluorescent Microscopy of the Mitochondrial Network

Cells were treated for 6 hours with 20 nM paclitaxel and then incubated with 25 mg/ml MitoTracker Red CMXRos (Molecular Probes, Saint Aubin, France) at 37°C for 20 minutes. To inhibit mitochondrial fission, we incubated cells for 6 hours with mdivi-1 (Sigma) at 1 μ mol/l, alone or simultaneously combined with paclitaxel. Cells were examined using a Leica DM-IRBE microscope coupled to a digital camera driven by MetaMorph software (Princeton Instruments, Trenton, NJ). At least 300 mitochondria were analyzed for each experimental condition, from three independent experiments.

Reverse Transcription–Polymerase Chain Reaction Analysis

Reverse transcription–polymerase chain reaction (RT-PCR) was conducted to amplify *bim* and β_2 -microglobulin (β_2m) transcript.

Total cellular RNA was extracted with the NucleoSpin RNA II Kit in accordance with the manufacturer's instructions (Macherey-Nagel, Hoerd, France), and 1 μ g of total RNA was used for RT with random primers. The PCR conditions included a denaturing step at 93°C for 4 minutes, followed by 25 (for β_2m) and 34 (for *bim*) cycles of denaturation at 93°C for 30 seconds, annealing at 55°C for 30 seconds, and elongation at 72°C for 30 seconds. We verified that the amplifications were in the linear range. Amplified products were separated by electrophoresis on a 2% agarose gel. DNA bands were visualized by ethidium bromide staining, and the image was then digitized. The level of *bim* expression was normalized to β_2m transcript [relative expression level (REL)]. The percentages of variation of *bim* reported in the text were the mean values of three experiments.

Microarray Analysis

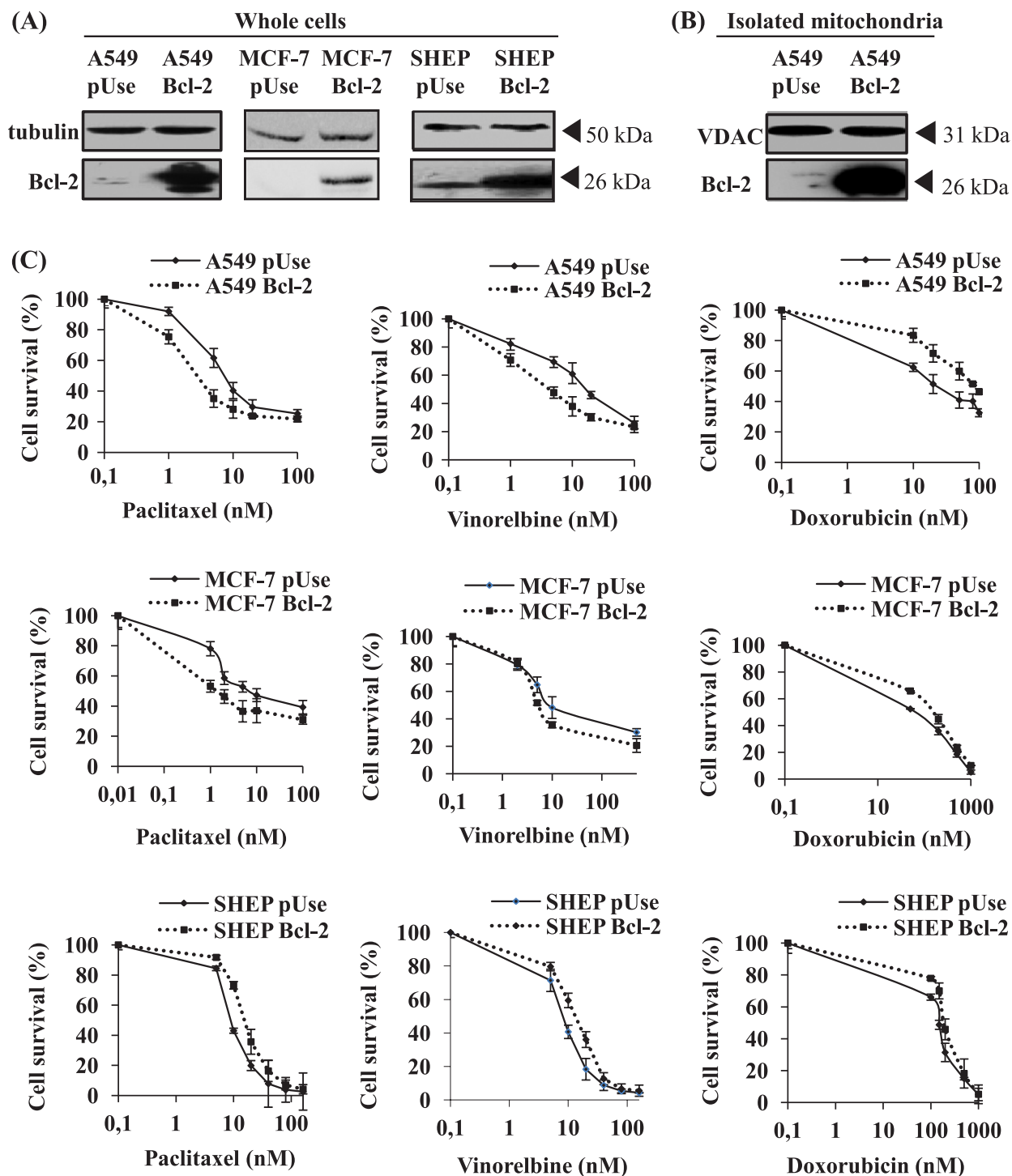
Total cellular RNA was isolated using the RNeasy Mini Kit (Qiagen) according to the manufacturer's instructions. Total RNA was checked for quantity, purity, and integrity by capillary electrophoresis using the Agilent 2100 Bioanalyzer and Agilent RNA Nano 6000 LabChip kits (Agilent Technologies, Palo Alto, CA). All the RNA samples presented an RNA integrity number of 10.0. Overall changes in gene expression were evaluated using the Agilent Two-Color Microarray-Based Gene Expression Platform using the Whole Human (V2) Gene Expression microarray 4 \times 44K 60-mer oligonucleotide (Agilent Technologies). Four different RNA resulting from four different cell cultures of A549 pUse or A549 Bcl-2 were used to perform the hybridization on the four arrays. Two hundred nanograms of total RNA was used to prepare labeled cRNA with the Agilent Low Input Quick Amp Labeling Kit, Two Colors, according to the manufacturer's recommendations. cRNA yield and Cy3 and efficiency of Cy5 incorporation into the cRNA were determined using a NanoDrop ND-1000 spectrophotometer (NanoDrop Technologies, Palo Alto, CA). For each sample, a total of 825 ng of cRNA was fragmented using the Agilent Gene Expression Hybridization Kit, and then Cy3 cRNA from a A549 pUse sample and Cy5 cRNA from a A549 Bcl-2 sample were hybridized together on one array. The hybridization was performed in a hybridization oven (Robbins Scientific, Sunnybrook, CA) at 65°C at 10 rpm for 17 hours. Slides were scanned using an Agilent DNA microarray scanner at 5- μ m resolution and Cy3/Cy5 intensity data were extracted using Agilent's Feature Extraction software including quality control based on internal controls. Transcriptome analysis was performed using Agilent Genespring GX11 Software. Fold changes were calculated and genes with more than a two-fold difference and $P \leq .05$ (Benjamini-Hochberg false discovery rate (FDR) parametric statistical test) were selected for detailed analysis pathways.

Reporter Luciferase Assay

A549 pUse and Bcl-2 cells were transiently transfected using Lipofectamine 2000 (Invitrogen) with Bim-pGL3, corresponding to *bim* promoter DNA, connected to the firefly luciferase gene or with a Renilla control plasmid pGL4 (Promega, Madison, WI) to normalize the transfection efficiency.

Next, after 24 hours, a passive lysis was performed, and both firefly and *Renilla* luciferase activities were quantified using the dual luciferase reporter assay system (Promega) according to the manufacturer's instructions. Luciferase was quantified using a luminometer (TD-20/20; Turner Designs, Sunnyvale, CA).

The same experiment was performed with a pGL3 mutated on the two binding sites of FoxO3a, Bim-luc dm.



(D)

IC ₅₀ nM	A549 pUse	A549 Bcl-2	MCF-7 pUse	MCF-7 Bcl-2	SHEP pUse	SHEP Bcl-2
Paclitaxel	6 ± 1	3.0 ± 0.1 †	6 ± 1	3 ± 1 †	11 ± 1	17 ± 2 *
Vinorelbine	10 ± 2	6 ± 1 †	7.0 ± 0.5	5.0 ± 0.2 †	10 ± 2	16 ± 3 *
doxorubicin	26 ± 5	135 ± 15 *	58 ± 7	110 ± 20 †	105 ± 5	152 ± 7 †

Statistical Analysis

Each experiment was performed at least in triplicate. Data were expressed as means \pm SEM. Statistical significance was tested using Student's *t* test for comparisons between means. A significant difference between two conditions was recorded for $P < .05$ or $P < .01$. Kaplan-Meier survival curves were plotted using GraphPad Prism 4 (GraphPad Software, San Diego, CA) and analyzed using the log-rank (Mantel-Cox) test.

Results

MTAs Exert Higher Antiproliferative Effects in Bcl-2–Overexpressing Lung and Breast Carcinoma Cells

We selected three tumor cell lines for their different tissue origins (lung, breast, and neuroblastoma). From these different cell lines, we generated various cellular models overexpressing Bcl-2 to investigate the role of Bcl-2 in the anticancer activity of MTAs. Protein expression levels were measured in whole cells to verify transfection success (Figure 1A) and in isolated mitochondria to ensure Bcl-2 functional localization (Figure 1B for A549; data not shown for MCF-7 and SHEP). We verified that with no treatment, doubling times of Bcl-2–overexpressing cells were not modified compared with pUse-transfected cells (Figure W1).

The impact of Bcl-2 overexpression on MTA activities was first evaluated with cell proliferation assays in lung carcinoma A549 cells. Paclitaxel antiproliferative efficacy was doubled in A549 Bcl-2 cells than in A549 pUse cells, as indicated by 50% inhibition of surviving fraction (IC_{50}) values ($P < .05$; Figure 1, C and D). Analysis of cell cycle distribution was also performed after a 24-hour paclitaxel treatment (Figure W2) and showed that accumulation in the G_2/M phase was higher in A549 Bcl-2 cells than in A549 pUse cells ($46.1 \pm 6.4\%$ versus $34.3 \pm 3.5\%$; $P < .05$). The increase in sensitivity of A549 cells that overexpress Bcl-2 was similarly measured with vinorelbine treatment (Figure 1C). Enhanced MTA activity was confirmed in another clone of A549 Bcl-2 cells (Figure W3, A and B). The higher sensitivity of A549 Bcl-2 cells may be specific to MTAs, because they display a significant resistance to the DNA-damaging agent doxorubicin (2.9-fold, $P < .05$) (Figure 1, C and D). The use of siRNA directed against Bcl-2 partly reversed A549 Bcl-2 cell sensitivity to paclitaxel ($IC_{50} = 16 \pm 6$ nM in siRNA control cells versus 38 ± 5 nM in siRNA Bcl-2 cells; Figure 2), definitely linking high Bcl-2 levels with higher treatment efficacy.

We then performed the proliferation assays in breast carcinoma cells. As shown in Figure 1, C and D, both paclitaxel and vinorelbine were more active in MCF-7 Bcl-2 cells than in MCF-7 pUse cells ($P < .05$). As in A549 cells, the enhanced treatment cytotoxicity may be specific to MTAs, because doxorubicin efficacy was decreased in Bcl-2 overexpressing MCF-7 cells (two-fold, $P < .05$; Figure 1, C and D).

In sharp contrast, Bcl-2 overexpression resulted in resistance of neuroblastoma SHEP cells to both paclitaxel and vinorelbine ($P <$

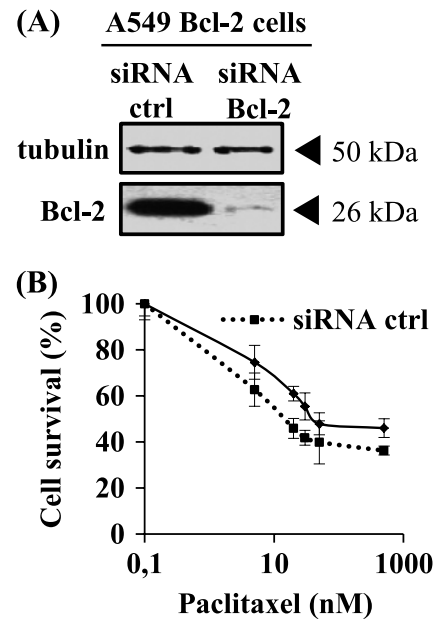


Figure 2. siRNA directed against Bcl-2 partly reversed A549 Bcl-2 cell sensitivity to paclitaxel. (A) Reduced Bcl-2 expression was verified by Western blot analysis on whole-cell lysates of A549 48 hours after transfection. Tubulin was used as a loading control. (B) Cytotoxicity of paclitaxel (48-hour treatment) was measured using an MTT assay.

.01). These results clearly indicate that the role of Bcl-2 in potentiating MTA efficacy is cell type dependent but is not limited to lung cancer cells. Furthermore, our preliminary work showed that overexpression of Bcl-2 did not enhance paclitaxel cytotoxicity in HBL100 non-cancer breast cells ($IC_{50} = 25$ nM for both HBL100 pUse and Bcl2 cells; data not shown).

Bcl-2 Overexpression Enhances In Vivo Lung Cancer Sensitivity to Paclitaxel

The role of Bcl-2 in the antitumor activity of MTAs was further evaluated *in vivo*, in nude mice bearing human lung carcinoma cell xenografts. Animals were treated with paclitaxel or vehicle (control), by i.v. injections for 5 days. As shown in Figure 3A, in the vehicle-treated cohort, A549 Bcl-2 tumor growth was unchanged compared with A549 pUse tumor growth (respectively 1323 ± 295 mm³ and 1307 ± 214 mm³ at experiment completion). This result shows that the increase in Bcl-2 expression level did not enhance A549 tumor progression.

Interestingly, 56 days after the start of treatment with paclitaxel, the mean tumor volume was 2.4 times smaller in mice xenografted with A549 Bcl-2 cells than with A549 pUse cells ($P < .05$; Figure 3A). Bcl-2 overexpression also appeared effective in improving treatment activity in terms of survival benefits: It led to a substantial increase in

Figure 1. Overexpression of Bcl-2 in A549 and MCF-7 cells increased their sensitivity to MTAs. (A) Bcl-2 overexpression was verified by Western blot analysis on whole-cell lysates of A549, MCF-7, and SHEP cells and on mitochondria isolated from A549 cells (B). Tubulin or VDAC expression was used as a loading control. (C) Cytotoxicity of paclitaxel, vinorelbine, and doxorubicin (72-hour treatment) was measured using an MTT assay in A549, MCF-7, and SHEP cells. (D) IC_{50} values were graphically determined from at least three independent experiments for each drug and each cell line (* $P < .01$, [†] $P < .05$).

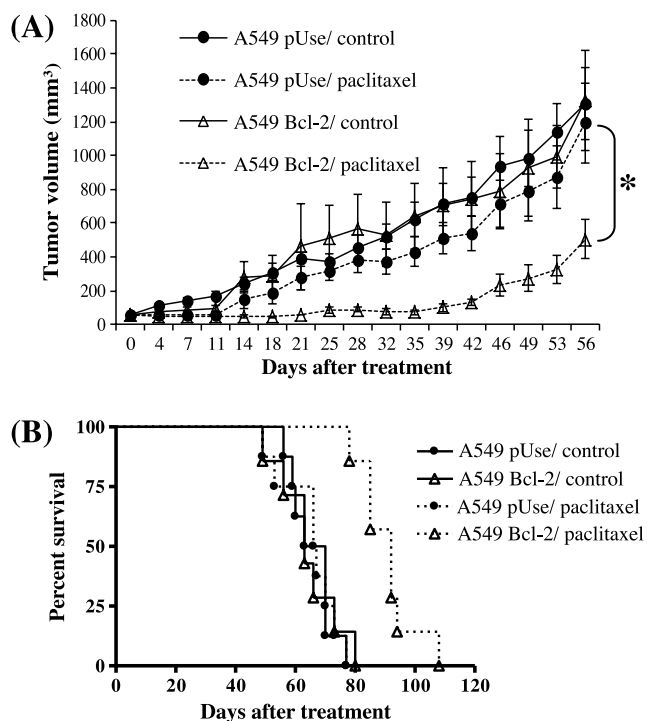


Figure 3. Overexpression of Bcl-2 enhances A549 lung cancer sensitivity to paclitaxel *in vivo*. (A) Tumor volumes in A549 pUse or A549 Bcl-2 cell-bearing mice receiving i.v. injection of vehicle (control) or paclitaxel ($P < .05$). Tumors were measured twice a week for 56 days after the initial treatment (day 0). (B) Kaplan-Meier curves showing survival in paclitaxel-treated A549 pUse or A549 cell-bearing mice compared with controls.

median survival, from 67 days in the cohorts of A549 pUse animals to 92 days in A549 Bcl-2 animals ($P < .005$; Figure 3B). Taken together, these *in vivo* data are consistent with the *in vitro* results. They clearly show that Bcl-2 overexpression is able to increase treatment efficacy in lung cancers.

Bim Up-Regulation Is Responsible for the Enhanced Efficacy of MTAs in Bcl-2-Overexpressing Cells

To understand how Bcl-2 can enhance lung tumor sensitivity to treatment, we performed cDNA microarrays to identify differentially expressed genes between A549 Bcl-2 cells and A549 pUse cells (Figure 4A). As expected, Bcl-2 gene expression was considerably increased in A549 Bcl-2 cells (48-fold, $P < .05$). We then analyzed the expression of other Bcl-2 family members known to be involved in MTA-induced apoptosis [39]. Gene expression profiles of most of them were not significantly modified in Bcl-2-overexpressing cells (Figure 4A). In particular, there was no variation in mRNA levels of A1, Mcl-1, and Bcl-XL antiapoptotic proteins. Expression levels of the proapoptotic actors Bax, Bak, Puma, Noxa, and Bmf were either not modified or decreased, so they could not be responsible for the higher sensitivity of A549 Bcl-2 cells to treatment. However, increase in mRNA levels of both Bad (1.3-fold) and *bim* (2.5-fold) was detected in A549 Bcl-2 cells *versus* A549 pUse cells ($P < .05$).

We thus focused our attention on Bim, a proapoptotic member of the Bcl-2 family, which 1) underwent the highest change in expression and 2) is able to bind to microtubules and to be released toward

mitochondria by MTAs [24]. The unexpected Bim overexpression in A549 Bcl-2 cells was first confirmed by RT-PCR (Figure 4B) and by Western blot (Figure 4C, left panel). These results were concomitantly validated in another clone of A549 Bcl-2 cells (Figure W3C). In addition, Bim overexpression in A549 Bcl-2 cells was reversed by Bcl-2 silencing (Figure 4D), confirming that this process is Bcl-2 dependent. Bim up-regulation was not specific to lung cancer cells, because similar variations were measured in breast MCF-7 Bcl-2 cells (data not shown). In sharp contrast, in SHEP cells overexpressing Bcl-2, in which a classic resistance to MTAs was observed, no overexpression of Bim was detected, either at mRNA or protein level (Figure 4, B and C, right panel). Considering the response of the three cell types to treatments (see above), our data strongly suggest that Bim expression level may control cell sensitivity to treatment.

This hypothesis was supported by the finding that Bim silencing suppressed the gain in treatment efficacy (Figure 5, A and B). Paclitaxel IC_{50} value was 2.5 times higher in A549 Bcl-2 cells transfected with Bim siRNA than in control siRNA-transfected ones ($P < .05$). The hypothesis was also supported by *bim* cDNA transfer in A549 wild-type cells (Figure 5C), which enhanced paclitaxel efficacy (IC_{50} decreased from 32 ± 6 nM in A549 pcDNA₆ cells to 20 ± 1 nM in A549 pcDNA₆-Bim cells, data not shown). The present study thus shows that Bim up-regulation, mediated by Bcl-2 overexpression in lung and breast cancer cells, is responsible for the unexpected improved response to treatment.

The Increase in bim Promoter Transcriptional Activity Is FoxO Dependent

Increase in *bim* mRNA levels in Bcl-2-overexpressing cells suggests the establishment of a transcriptional regulation. We examined this hypothesis using a reporter gene construct containing a firefly luciferase under the control of the wild-type *bim* promoter (Bim-pGL3). As shown in Figure 6A, *bim* promoter transcriptional activity was increased 2.3 ± 0.2 -fold in A549 Bcl-2 cells *versus* A549 pUse cells ($P < .01$).

Bim mRNA expression is mainly regulated by FoxO3a, a member of the FoxO family of transcription factors. We first studied FoxO3a localization, because it must reside in the nucleus to bind to its cognate DNA targeting sequences. By confocal microscopy, we showed that FoxO3a was mainly present in the cytoplasm of A549 pUse cells, while it partly colocalized with the nucleus in A549 Bcl-2 cells (Figure 6B). Consistent with this finding, FoxO3a was more active in A549 Bcl-2 cells, as indicated by the increase in MnSOD mRNA level, a well-known target of the transcription factor, measured by DNA microarray (1.8-fold, $P < .05$, data not shown) and confirmed by RT-PCR (Figure 6C). This same target is not activated in SHEP Bcl-2 cells (Figure 6C).

Additionally, the DNA microarray analysis, confirmed by RT-PCR (Figure 6C), revealed that SGK2 mRNA was decreased in A549 Bcl-2 cells compared with A549 pUse cells (3.1-fold, $P < .05$, data not shown). Since SGK can inhibit FoxO3a nuclear translocation by phosphorylation, a reduction in its level may explain FoxO3a activation in A549 Bcl2 cells.

To further investigate the role of FoxO3a in Bim up-regulation, we transfected A549 Bcl-2 cells with Bim-pGL3 dm, a double mutant *Bim*-LUC reporter construct that contains mutations in the *bim1* and *bim2* FoxO sites. In these cells, we recorded a 2.7-fold decrease in *bim* promoter transcriptional activity (Figure 6D). Taken together,

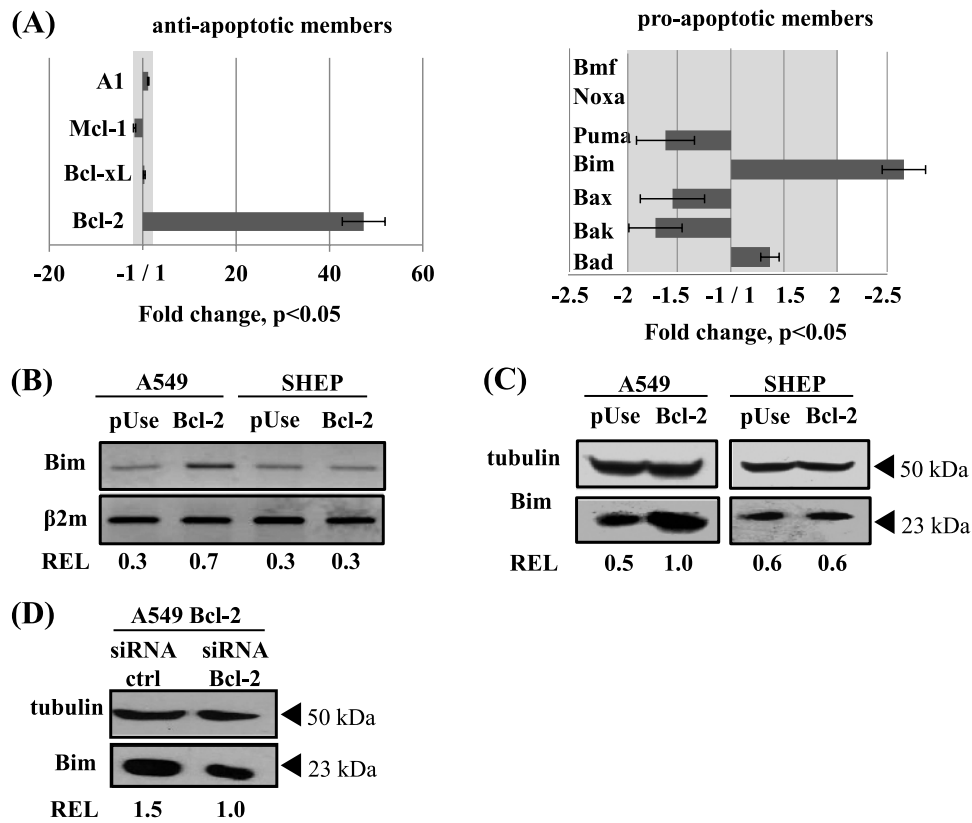


Figure 4. *Bim* mRNA and protein expression is induced in Bcl-2–overexpressing A549 cells. (A) Differences in gene expression profiles of Bcl-2 family members in A549 Bcl-2 cells versus A549 pUse cells, using DNA microarray analysis. Protein expression change in the grayed part of the histogram is less than two-fold. (B) *Bim* mRNA expression was analyzed by RT-PCR and normalized to β 2m transcript (REL). Western blot analysis of Bim protein was performed in whole-cell lysates from A549, SHEP (C), and A549 Bcl-2 cells transfected with siRNA Bcl-2 (D). Transfection efficiency was thus verified after 24 hours, when adding drug in experiments. Tubulin expression was used as a loading control to determine REL.

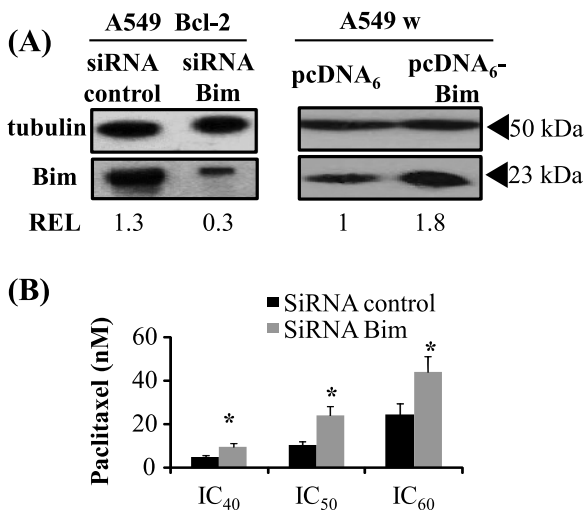


Figure 5. Bim expression level controls cell sensitivity to paclitaxel. (A) A549 Bcl-2 cells were transfected with either siRNA control or siRNA Bim. A549 wild-type cells (A549 w) were transfected with pcDNA₆ or pcDNA₆-Bim. Transfection efficiency was verified by Western blot analysis at 24 hours, when adding drug in experiments. (B) Cytotoxicity of a 48-hour paclitaxel treatment was evaluated in A549 Bcl-2 cells transfected with siRNA control and siRNA Bim (**P* < .05).

our results clearly demonstrate that Bim transcriptional regulation, mediated by Bcl-2 overexpression, is FoxO3a dependent.

Bim-Mediated Increase in Cell Sensitivity to Treatment Is Linked to Mitochondrial Network Disruption

To decipher the functional consequences of Bim up-regulation in Bcl-2–overexpressing cells, we first checked that the mitochondrial membranes were permeabilized, a key step in the MTA mechanism of action. First, we recorded an increase in the mitochondrial reducing potential in A549 Bcl-2 cells after a short-time treatment with paclitaxel (6 hours, *P* < .05), whereas it did not vary in A549 pUse cells (Figure W4A). We then observed the release of cytochrome *c* from mitochondria after a 24-hour treatment with paclitaxel (Figure W4B). Lastly, we detected caspase-9 activation, indicated by the cleavage of the pro-caspase-9 in a dose- and time-dependent manner (Figure W4C). Taken together, these assays confirmed that paclitaxel activates the mitochondrial apoptotic pathway in lung cancer cells that express high levels of Bim, even though cells also overexpress Bcl-2.

Morphology of mitochondria is crucial for maintaining their functions and depends on the balance between fission and fusion. We thus investigated the impact of paclitaxel on the mitochondrial network morphology by fluorescence microscopy. As expected, untreated cells displayed elongated tubular mitochondria (Figure 7, A and B, left panels), and paclitaxel disturbed the mitochondrial network fission/

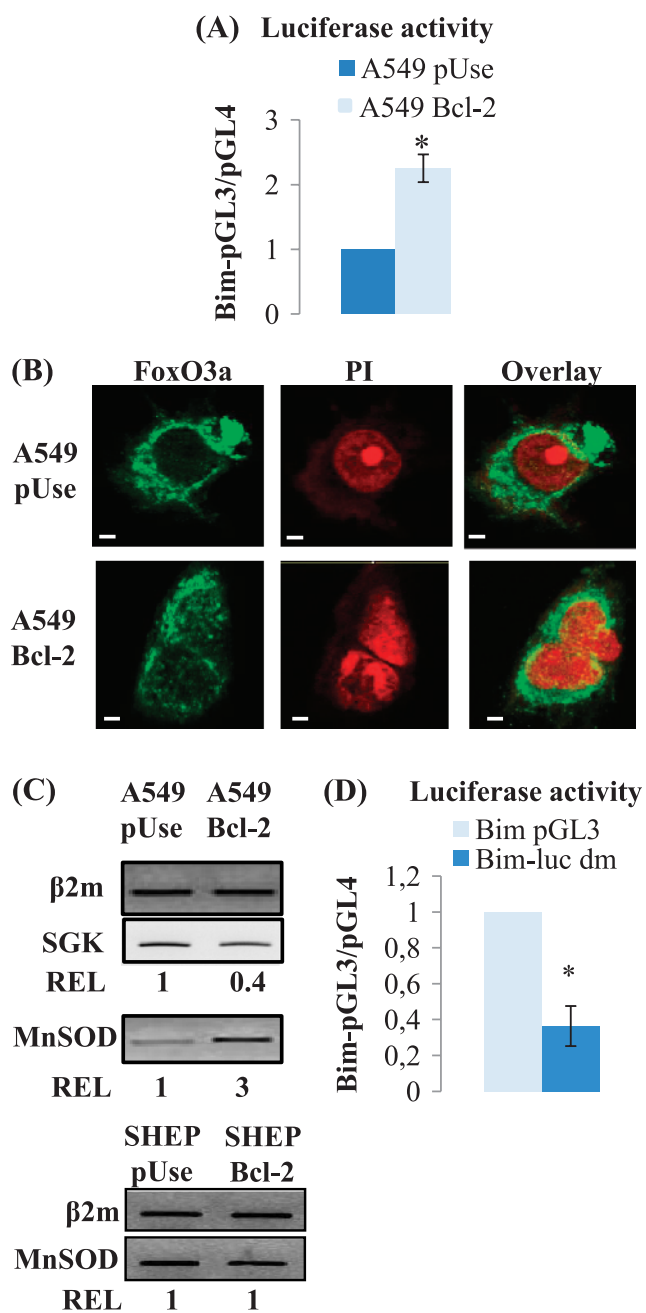


Figure 6. Bim expression in Bcl-2–overexpressing cells is modulated by FoxO3a. (A) Luciferase activity was measured in A549 pUse and A549 Bcl-2 cells. (B) FoxO3a colocalized with the nucleus, stained with propidium iodide (PI), in A549 Bcl-2 cells, and remained only cytoplasmic in A549 pUse cells (scale bars, 10 μ m). (C) RT-PCR analysis of MnSOD and SGK mRNA expression. (D) Luciferase activity in A549 Bcl-2 cells transfected with a FoxO-mutated binding site *bim* promoter construct (Bim-luc dm) compared with the wild-type plasmid.

fusion balance. Both A549 pUse and SHEP pUse cells displayed spherical organelles after a short-time treatment (Figure 7, *A* and *B*, *right panels*). More interestingly, by quantifying cells with a fragmented mitochondrial network, we revealed a three-fold increase in this process in A549 Bcl-2 cells compared with A549 pUse cells ($P < .05$). By contrast, paclitaxel-mediated fragmentation of the mitochondrial network was not enhanced in SHEP Bcl-2 cells ($60 \pm 4\%$) compared with SHEP pUse cells ($66 \pm 4\%$).

To further study the mechanisms underlying the mitochondrial network fragmentation induced by paclitaxel, we evaluated the role of Drp1, a key actor of mitochondrial fission. The pharmacological inhibitor of Drp1 (mdivi-1) reduced the quantity of A549 Bcl-2 cells with punctuated mitochondria from $42 \pm 7\%$ to $28 \pm 1\%$ ($P < .05$; Figure 7, *A* and *C*). Concomitantly, the cytotoxic effect of paclitaxel (IC_{70}) was decreased 1.7-fold when simultaneously combined with mdivi-1, indicating that treatment efficacy in A549 Bcl-2 cells was related to the promotion of mitochondrial fission.

Finally, to determine whether Bcl-2–mediated up-regulation of Bim could be responsible for mitochondrial fission, we tested the effect of Bim silencing on this process. After paclitaxel treatment, the proportion of cells that displayed a fragmented mitochondrial network decreased from $65 \pm 3\%$ in siRNA control cells to $41 \pm 5\%$ in *bim* siRNA–transfected cells ($P < .01$; Figure 7*D*). Thus, Bim silencing leads to resistance of A549 Bcl-2 cells to paclitaxel by an mdivi-1–like inhibition of mitochondrial fission. Our results thus highlight Bim involvement in the enhanced sensitivity of Bcl-2–overexpressing cells by disrupting the mitochondrial network dynamics and functions in lung cancer cells.

Discussion

Accumulating evidence from preclinical studies and clinical trials suggests that targeted therapies that work by downregulating Bcl-2 may not be potent in increasing the efficacy of some conventional chemotherapies. In the present study, we show for the first time the involvement of Bim in MTA efficacy, supporting interest in BH3-mimetic strategies to improve treatment of lung cancers and overcome drug resistance.

The aim of our work was to evaluate response to treatment for tumors that intrinsically overexpress Bcl-2. The study design, by gene transfer in tumor cells, enables us to efficiently induce Bcl-2 overexpression, as observed in many patients, including those bearing lung cancers [30]. To date, up-regulation of the prosurvival protein Bcl-2 remains widely considered as a mechanism involved in tumor cell resistance to MTAs [14,40]. However, in Bcl-2–overexpressing lung and breast cells, we showed here that paclitaxel and vinorelbine activities were increased. In the literature, previous *in vitro* studies highlighted a role for Bcl-2 in cell sensitivity to MTAs. In particular, Bcl-2 up-regulation resulted in the enhanced sensitivity of lung cancer cells to docetaxel [19]. High expression levels of Bcl-2 in breast and ovarian cancer cells are also linked to a higher sensitivity to vinca alkaloids and paclitaxel [21,22,31]. Thus, patients with Bcl-2 positive tumors may be MTA responsive.

Interestingly, Bcl2 protein was detected in metaplasia and increased with the development of malignancy, while it was expressed in any normal lung specimens [41]. Hence, we can assume that Bcl-2–overexpressing tumor cells are more sensitive to MTAs than surrounding normal cells, which may help improve patient care.

In the present study, we further validated *in vivo* this dual role for Bcl-2 in MTA treatment potency, using mouse models bearing Bcl-2–overexpressing non–small cell lung xenografts.

Interestingly, we revealed that Bcl-2 overexpression selectively induced the expression of the mitochondrial proapoptotic Bim, resulting in the increased sensitivity of cancer cells to MTAs. In addition, siRNA directed against Bcl-2 restored the basal expression level of Bim and the standard response to treatment. This may help to explain why high expression levels of Bcl-2 can correlate with favorable clinical outcomes for patients with several types of cancer [42,43].

Bound in an inactive form to microtubules through the dynein light chain [26], Bim accumulates in mitochondria to trigger membrane permeabilization. It has been shown to play a major role in paclitaxel and epothilone-induced cancer cell death [23,24]. This involvement of signaling associated with disturbances of the microtubule system could

explain why the higher sensitivity of Bcl-2-overexpressing cells may be specific to MTAs.

How Bcl-2 overexpression in turn causes the increase in *bim* mRNA amounts remains unanswered. In 2007, Jorgensen et al. showed that Bcl-2 and Bim could control each other's expression in

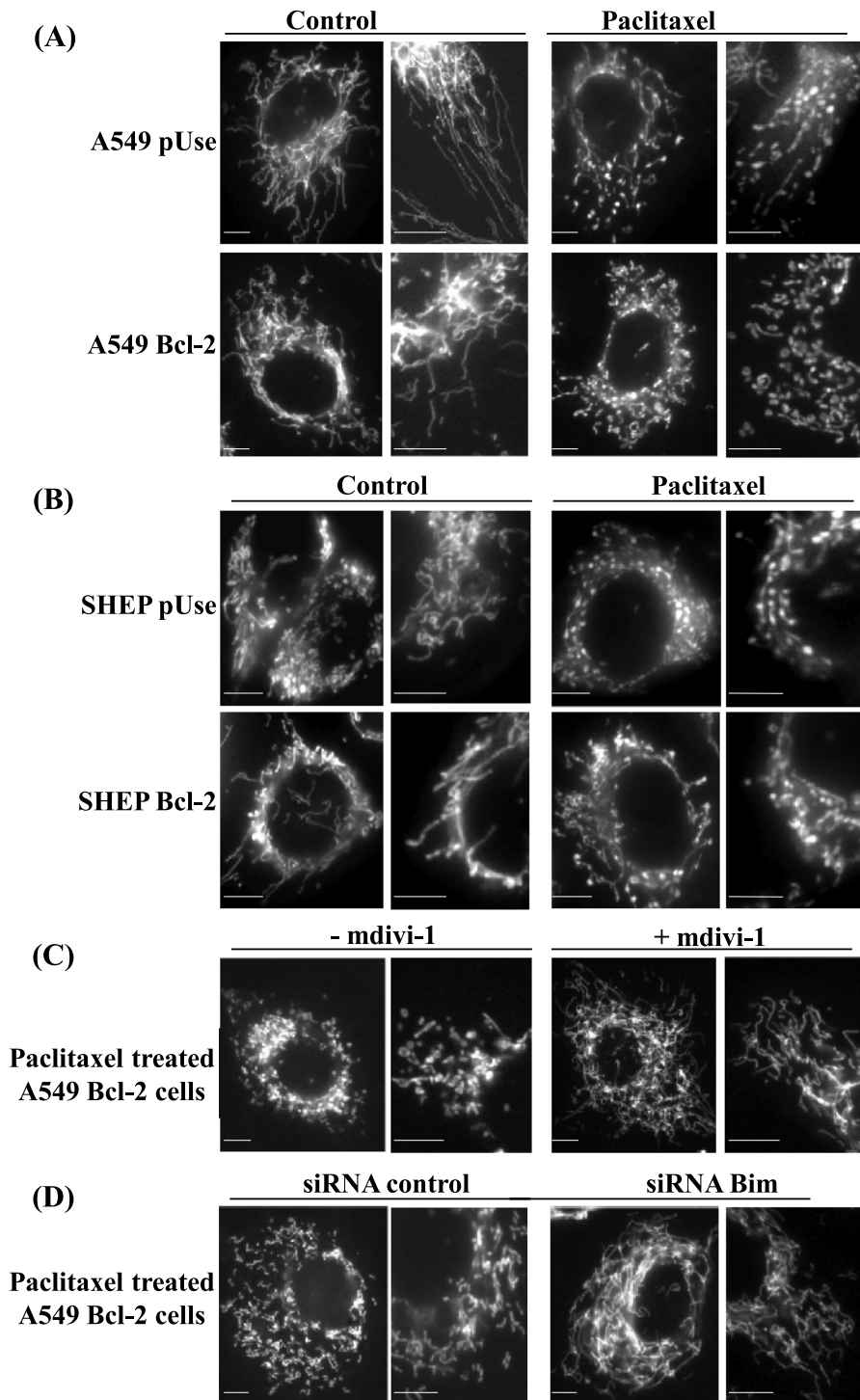


Figure 7. Paclitaxel efficacy involves a Bim-mediated mitochondrial network fragmentation. (A) Mitochondrial morphology in A549 pUse and A549 Bcl-2 cells, untreated or treated with paclitaxel IC₇₀ for 6 hours. The right-hand photos are magnifications of a localized zone. (B) Same experiments in SHEP pUse and Bcl-2 cells. (C) Similar experiments in A549 Bcl-2 cells treated with paclitaxel alone or combined with the Drp1 inhibitor mdivi-1. (D) Same experiments after a 6-hour treatment with paclitaxel in A549 Bcl-2 cells transfected with the siRNA control or the siRNA directed against Bim. Scale bars, 10 μm.

T cells [44]. In particular, they described that Bcl-2 overexpression, through a transgene, raised intracellular amounts of Bim. Up to now, there has been no evidence of any transcription factor that could activate Bim in response to Bcl-2. In our study, we propose an explanation for the Bcl-2-governed Bim up-regulation. Many studies have described the central role played by FoxO3a in Bim transcriptional regulation, including in paclitaxel-treated cancer cells [27]. We confirm here its implication by using a *bim* promoter plasmid carrying two mutated FoxO binding sites. Inhibition of SGK has been linked to a decrease in FoxO3a phosphorylation, which results in its activation through its relocalization from cytosol to nucleus [28,29]. Our data support the triggering of such a signaling pathway in Bcl-2-overexpressing A549 cells, since we recorded a decrease in SGK mRNA levels, visualized FoxO3a nuclear accumulation, and measured the up-regulation of its well-known target MnSOD. Furthermore, we previously showed that Bcl-2 inhibits the transcriptional activity of p53 [45,46], which could lead to a decrease in SGK expression [47,48]. In response to Bcl-2 overexpression, we thus hypothesize that Bim is upregulated as a result of the increase in FoxO3a activity, allowed by p53 and SGK inhibition. Unlike the A549 cell line, we can infer that the SGK-FoxO3a pathway is not involved in SHEP cell line, since neither Bim nor MnSOD is upregulated. When activated in neuroblastoma cells, FoxO3a is able to trigger a Bim-mediated cell death [49], and the reason why MTAs failed in inducing this process remains to be deciphered.

The functional consequences of Bim overexpression in cancer cells have been well documented. Bim triggers the release of proapoptotic mediators from mitochondria to cytosol, a key step in the cell death program [5]. Previous work also suggests that mitochondrial fragmentation may be required in this process [6]. In the present study, Bim silencing prevented mitochondrial fragmentation and reversed paclitaxel sensitivity in Bcl-2-overexpressing lung cells. The precise molecular mechanisms leading to drug-mediated mitochondrial fragmentation are not fully understood, but there is evidence that this process can result from actions of Bcl-2 family members on the mitochondrial fission/fusion machinery [10,11]. In the present study, we found that Bim was involved in the paclitaxel-mediated mitochondrial network fragmentation. Interestingly, a recent study also showed that the BH3-mimetic ABT-737 led to a widespread fragmentation of mitochondria in neurons [50]. Consistent with this finding, treatment of mouse embryonic fibroblasts with the death domain of Bim induced mitochondria to undergo fission, by increasing Bcl-xL binding with Drp1 [51]. We show here that Drp1 inhibition decreased drug efficacy, supporting a role for mitochondrial fission in inhibiting cancer cell expansion. Another study in A549 cells confirm this hypothesis by showing that mitochondrial fission defects contribute to apoptotic resistance in A549 cells [52].

Lastly, our data strongly suggest that cell sensitivity status is monitored by Bim expression level rather than Bcl-2 expression level. Preliminary unpublished data on several malignant breast cell lines confirm that cell sensitivity to paclitaxel was correlated with Bim expression levels. Sensitivity to paclitaxel is greater in high Bim-expressing cells (SKBR3) than in very low Bim-expressing cells (MDA-MB-231). If Bcl-2 overexpression does not lead to Bim up-regulation, then a classic resistance is measured, as in neuroblastoma cells. By contrast, when Bcl-2 overexpression induces Bim up-regulation, as observed in breast and lung carcinoma cells, then MTA efficacy is enhanced. Our findings are important in the current context of the development of targeted therapies directed toward Bcl-2. Several studies have proposed an expla-

nation for the lack of efficacy in combining oblimersen with some conventional chemotherapies. Moulder et al. have argued that oblimersen may not suppress intratumoral Bcl-2 levels sufficiently to affect chemotherapeutic sensitivity [18]. Rudin et al. have suggested that Bcl-2, although overexpressed, would not be a relevant biomarker [16]. Taken together, these data prompt new therapeutic approaches [53]. Recent advances include the discovery of small BH3-mimetic molecules, which inhibit antiapoptotic Bcl-2 proteins through their binding to the hydrophobic groove [25]. In particular, gossypol and ABT-737 have already shown their efficacy in lung cancer [54,55]. Recently, Oakes et al. have proved the efficacy of ABT-737 for the treatment of basal-like breast cancers with both elevated Bcl-2 and Bim levels [56]. Similarly, a recent study suggests the possibility that the loss of Bim expression in non-small cell lung cancer might be related to resistance to anticancer drugs [57]. Thus, targeting or overexpressing BH3-only proteins such as Bim may be a strategy of choice to improve treatment efficacy and overcome drug resistance to cancer chemotherapy.

To conclude, by showing for the first time a Bcl-2-governed Bim induction, we offer an explanation for the favorable higher sensitivity of Bcl-2-overexpressing cells to MTAs. Our work highlights that rather than Bcl-2 status alone, Bim expression pattern should be determined to predict cell sensitivity to MTA. It would be interesting to realize tissue microarray (TMA) studies to help validate this biomarker in clinical practice. Considering the growing importance of Bim function as a mediator of apoptosis, the understanding of its gene regulation and cellular behavior is now an essential objective.

Acknowledgments

The authors thank C. Ferlini (Rome, Italy) for the Bcl-2 pUse and the empty plasmids, A. Vasquez (Paris, France) for the pcDNA₆ and pcDNA₆-Bim, and J. Ham (London, United Kingdom) for the Bim-pGL3 and Bim-luc dm. The authors also thank Charles Prevôt for technical assistance in flow cytometry analysis, Elise Termine (Genomic Platform IFR125, Marseille, France) for microarray analysis, and Alain Desobry for technical assistance.

References

- Estève M-A, Carré M, and Braguer D (2007). Microtubules in apoptosis induction: are they necessary? *Curr Cancer Drug Targets* **7**, 713–729.
- Honore S, Pasquier E, and Braguer D (2005). Understanding microtubule dynamics for improved cancer therapy. *Cell Mol Life Sci* **62**, 3039–3056.
- Rovini A, Carré M, Bordet T, Pruss RM, and Braguer D (2010). Olesoxime prevents microtubule-targeting drug neurotoxicity: selective preservation of EB comets in differentiated neuronal cells. *Biochem Pharmacol* **80**, 884–894.
- André N, Carré M, Brasseur G, Pourroy B, Kovacic H, Briand C, and Braguer D (2002). Paclitaxel targets mitochondria upstream of caspase activation in intact human neuroblastoma cells. *FEBS Lett* **532**, 256–260.
- Akiyama T, Dass CR, and Choong PFM (2009). Bim-targeted cancer therapy: a link between drug action and underlying molecular changes. *Mol Cancer Ther* **8**, 3173–3180.
- Youle RJ and Karbowski M (2005). Mitochondrial fission in apoptosis. *Nat Rev Mol Cell Biol* **6**, 657–663.
- Cassidy-Stone A, Chipuk JE, Ingerman E, Song C, Yoo C, Kuwana T, Kurth MJ, Shaw JT, Hinshaw JE, Green DR, et al. (2008). Chemical inhibition of the mitochondrial division dynamin reveals its role in Bax/Bak-dependent mitochondrial outer membrane permeabilization. *Dev Cell* **14**, 193–204.
- Smirnova E, Griparic L, Shurland DL, and Van der Bliek AM (2001). Dynamin-related protein Drp1 is required for mitochondrial division in mammalian cells. *Mol Biol Cell* **12**, 2245–2256.
- Sheridan C and Martin SJ (2010). Mitochondrial fission/fusion dynamics and apoptosis. *Mitochondrion* **10**, 640–648.
- Autret A and Martin SJ (2009). Emerging role for members of the Bcl-2 family in mitochondrial morphogenesis. *Mol Cell* **36**, 355–363.

- [11] Cleland MM, Norris KL, Karbowski M, Wang C, Suen D-F, Jiao S, George NM, Luo X, Li Z, and Youle RJ (2011). Bcl-2 family interaction with the mitochondrial morphogenesis machinery. *Cell Death Differ* **18**, 235–247.
- [12] Michaud WA, Nichols AC, Mroz EA, Faquin WC, Clark JR, Begum S, Westra WH, Wada H, Busse PM, Ellisen LW, et al. (2009). Bcl-2 blocks cisplatin-induced apoptosis and predicts poor outcome following chemoradiation treatment in advanced oropharyngeal squamous cell carcinoma. *Clin Cancer Res* **15**, 1645–1654.
- [13] Sartorius UA and Krammer PH (2002). Upregulation of Bcl-2 is involved in the mediation of chemotherapy resistance in human small cell lung cancer cell lines. *Int J Cancer* **97**, 584–592.
- [14] Tabuchi Y, Matsuoka J, Gunduz M, Imada T, Ono R, Ito M, Motoki T, Yamatsuji T, Shirakawa Y, Takaoka M, et al. (2009). Resistance to paclitaxel therapy is related with Bcl-2 expression through an estrogen receptor mediated pathway in breast cancer. *Int J Oncol* **34**, 313–319.
- [15] O'Brien S, Moore JO, Boyd TE, Larratt LM, Skotnicki AB, Koziner B, Chanan-Khan AA, Seymour JF, Gribben J, Itri LM, et al. (2009). 5-Year survival in patients with relapsed or refractory chronic lymphocytic leukemia in a randomized, phase III trial of fludarabine plus cyclophosphamide with or without oblimersen. *J Clin Oncol* **27**, 5208–5212.
- [16] Rudin CM, Salgia R, Wang X, Hodgson LD, Masters GA, Green M, and Vokes EE (2008). Randomized phase II study of carboplatin and etoposide with or without the bcl-2 antisense oligonucleotide oblimersen for extensive-stage small-cell lung cancer: CALGB 30103. *J Clin Oncol* **26**, 870–876.
- [17] Sternberg CN, Dumez H, Van Poppel H, Skoneczna I, Sella A, Daugaard G, Gil T, Graham J, Carpentier P, Calabro F, et al. (2009). Docetaxel plus oblimersen sodium (Bcl-2 antisense oligonucleotide): an EORTC multicenter, randomized phase II study in patients with castration-resistant prostate cancer. *Ann Oncol* **20**, 1264–1269.
- [18] Moulder SL, Symmans WF, Booser DJ, Madden TL, Lipsanen C, Yuan L, Brewster AM, Cristofanilli M, Hunt KK, Buchholz TA, et al. (2008). Phase I/II study of G3139 (Bcl-2 antisense oligonucleotide) in combination with doxorubicin and docetaxel in breast cancer. *Clin Cancer Res* **14**, 7909–7916.
- [19] Inoue Y, Gika M, Abiko T, Oyama T, Saitoh Y, Yamazaki H, Nakamura M, Abe Y, Kawamura M, and Kobayashi K (2005). Bcl-2 overexpression enhances *in vitro* sensitivity against docetaxel in non-small cell lung cancer. *Oncol Rep* **13**, 259–264.
- [20] Del Bufalo D, Biroccio A, Trisciuoglio D, Bruno T, Floridi A, Aquino A, and Zupi G (2002). Bcl-2 has differing effects on the sensitivity of breast cancer cells depending on the antineoplastic drug used. *Eur J Cancer* **38**, 2455–2462.
- [21] Ferlini C, Raspaglio G, Mozzetti S, Distefano M, Filippetti F, Martinelli E, Ferrandina G, Gallo D, Ranalletti FO, and Scambia G (2003). Bcl-2 down-regulation is a novel mechanism of paclitaxel resistance. *Mol Pharmacol* **64**, 51–58.
- [22] Estève M-A, Carré M, Bourgarel-Rey V, Kruczynski A, Raspaglio G, Ferlini C, and Braguer D (2006). Bcl-2 down-regulation and tubulin subtype composition are involved in resistance of ovarian cancer cells to vinflunine. *Mol Cancer Ther* **5**, 2824–2833.
- [23] Li R, Moudgil T, Ross HJ, and Hu H-M (2005). Apoptosis of non-small-cell lung cancer cell lines after paclitaxel treatment involves the BH3-only proapoptotic protein Bim. *Cell Death Differ* **12**, 292–303.
- [24] Khawaja NR, Carré M, Kovacic H, Estève MA, and Braguer D (2008). Patupilone-induced apoptosis is mediated by mitochondrial reactive oxygen species through Bim relocalization to mitochondria. *Mol Pharmacol* **74**, 1072–1083.
- [25] Kang MH and Reynolds CP (2009). Bcl-2 inhibitors: targeting mitochondrial apoptotic pathways in cancer therapy. *Clin Cancer Res* **15**, 1126–1132.
- [26] Puthalakath H, Huang DC, O'Reilly LA, King SM, and Strasser A (1999). The proapoptotic activity of the Bcl-2 family member Bim is regulated by interaction with the dynein motor complex. *Mol Cell* **3**, 287–296.
- [27] Sunter A, Fernández de Mattos S, Stahl M, Brosens JJ, Zoumpoulidou G, Saunders CA, Coffer PJ, Medema RH, Coombes RC, and Lam EW (2003). FoxO3a transcriptional regulation of Bim controls apoptosis in paclitaxel-treated breast cancer cell lines. *J Biol Chem* **278**, 49795–49805.
- [28] Brunet A, Bonni A, Zigmond MJ, Lin MZ, Juo P, Hu LS, Anderson MJ, Arden KC, Blenis J, and Greenberg ME (1999). Akt promotes cell survival by phosphorylating and inhibiting a Forkhead transcription factor. *Cell* **96**, 857–868.
- [29] Brunet A, Park J, Tran H, Hu LS, Hemmings BA, and Greenberg ME (2001). Protein kinase SGK mediates survival signals by phosphorylating the Forkhead transcription factor FKHRL1 (FOXO3a). *Mol Cell Biol* **21**, 952–965.
- [30] Zhang H, Yousem SA, Franklin WA, Elder E, Landreneau R, Ferson P, Keenan R, Whiteside T, and Levitt ML (1998). Differentiation and programmed cell death-related intermediate biomarkers for the development of non-small cell lung cancer: a pilot study. *Hum Pathol* **29**, 965–971.
- [31] Del Bufalo D, Biroccio A, Leonetti C, and Zupi G (1997). Bcl-2 overexpression enhances the metastatic potential of a human breast cancer line. *FASEB J* **11**, 947–953.
- [32] Gao Q, Yang S, and Kang M-Q (2012). Influence of survivin and Bcl-2 expression on the biological behavior of non-small cell lung cancer. *Mol Med Report* **5**, 1409–1414.
- [33] Clybourn C, Hadji A, ELMchichi B, Auffredou M-T, Leca G, and Vazquez A (2009). BimL upregulation induced by BCR cross-linking in BL41 Burkitt's lymphoma results from a splicing mechanism of the BimEL mRNA. *Biochem Biophys Res Commun* **383**, 32–36.
- [34] Jordan MA, Toso RJ, Thrower D, and Wilson L (1993). Mechanism of mitotic block and inhibition of cell proliferation by taxol at low concentrations. *Proc Natl Acad Sci USA* **90**, 9552–9556.
- [35] Rose WC (1992). Taxol: a review of its preclinical *in vivo* antitumor activity. *Anticancer Drugs* **3**, 311–321.
- [36] Fujimoto S (1994). Study for modifying activity of solvents on antitumor activity of paclitaxel. *Gan To Kagaku Ryoho* **21**, 665–670.
- [37] Pasquier E, Carré M, Pourroy B, Camoin L, Rebaï O, Briand C, and Braguer D (2004). Antiangiogenic activity of paclitaxel is associated with its cytostatic effect, mediated by the initiation but not completion of a mitochondrial apoptotic signaling pathway. *Mol Cancer Ther* **3**, 1301–1310.
- [38] André N, Braguer D, Brasseur G, Gonçalves A, Lemesle-Meunier D, Guise S, Jordan MA, and Briand C (2000). Paclitaxel induces release of cytochrome *c* from mitochondria isolated from human neuroblastoma cells. *Cancer Res* **60**, 5349–5353.
- [39] Rovini A, Savry A, Braguer D, and Carré M (2011). Microtubule-targeted agents: when mitochondria become essential to chemotherapy. *Biochim Biophys Acta* **1807**, 679–688.
- [40] Chun E and Lee K-Y (2004). Bcl-2 and Bcl-xL are important for the induction of paclitaxel resistance in human hepatocellular carcinoma cells. *Biochem Biophys Res Commun* **315**, 771–779.
- [41] Kory PP, Zhang H, Franklin WA, Yousem SA, Landreneau R, and Levitt ML (2002). *In vivo* expression of p53 and Bcl-2 and their role in programmed cell death in premalignant and malignant lung lesions. *Lung Cancer* **35**, 155–163.
- [42] Uchida T, Minei S, Gao J-P, Wang C, Satoh T, and Baba S (2002). Clinical significance of p53, MDM2 and bcl-2 expression in transitional cell carcinoma of the bladder. *Oncol Rep* **9**, 253–259.
- [43] Anagnostou VK, Lowery FJ, Zolota V, Tzelepi V, Gopinath A, Liceaga C, Panagopoulos N, Frangia K, Tanoue L, Boffa D, et al. (2010). High expression of BCL-2 predicts favorable outcome in non-small cell lung cancer patients with non squamous histology. *BMC Cancer* **10**, 186.
- [44] Jorgensen TN, McKee A, Wang M, Kushnir E, White J, Refaeli Y, Kappler JW, and Marrack P (2007). Bim and Bcl-2 mutually affect the expression of the other in T cells. *J Immunol* **179**, 3417–3424.
- [45] Zhan Q, Kontny U, Iglesias M, Alamo I Jr, Yu K, Hollander MC, Woodworth CD, and Fornace AJ Jr (1999). Inhibitory effect of Bcl-2 on p53-mediated transactivation following genotoxic stress. *Oncogene* **18**, 297–304.
- [46] Bourgarel-Rey V, Savry A, Hua G, Carré M, Bressin C, Chacon C, Imbert J, Braguer D, and Barra Y (2009). Transcriptional down-regulation of Bcl-2 by vinorelbine: identification of a novel binding site of p53 on Bcl-2 promoter. *Biochem Pharmacol* **78**, 1148–1156.
- [47] Maiyar AC, Huang AJ, Phu PT, Cha HH, and Firestone GL (1996). p53 stimulates promoter activity of the *sgk* serum/glucocorticoid-inducible serine/threonine protein kinase gene in rodent mammary epithelial cells. *J Biol Chem* **271**, 12414–12422.
- [48] You H, Jang Y, You-Ten AI, Okada H, Liepa J, Wakeham A, Zaugg K, and Mak TW (2004). p53-dependent inhibition of FKHRL1 in response to DNA damage through protein kinase SGK1. *Proc Natl Acad Sci USA* **101**, 14057–14062.
- [49] Obexer P, Geiger K, Ambros PF, Meister B, and Auserlechner MJ (2007). FKHRL1-mediated expression of Noxa and Bim induces apoptosis via the mitochondria in neuroblastoma cells. *Cell Death Differ* **14**, 534–547.
- [50] Young KW, Piñón LGP, Dhiraj D, Twiddy D, Macfarlane M, Hickman J, and Nicotera P (2010). Mitochondrial fragmentation and neuronal cell death in response to the Bcl-2/Bcl-x(L)/Bcl-w antagonist ABT-737. *Neuropharmacology* **58**, 1258–1267.

- [51] Shroff EH, Snyder CM, Budinger GRS, Jain M, Chew T-L, Khuon S, Perlman H, and Chandel NS (2009). BH3 peptides induce mitochondrial fission and cell death independent of BAX/BAK. *PLoS One* **4**, e5646.
- [52] Thomas KJ and Jacobson MR (2012). Defects in mitochondrial fission protein dynamin-related protein 1 are linked to apoptotic resistance and autophagy in a lung cancer model. *PLoS One* **7**, e45319.
- [53] Nordigården A, Kraft M, Eliasson P, Labi V, Lam EW-F, Villunger A, and Jönsson JI (2009). BH3-only protein Bim more critical than Puma in tyrosine kinase inhibitor-induced apoptosis of human leukemic cells and transduced hematopoietic progenitors carrying oncogenic FLT3. *Blood* **113**, 2302–2311.
- [54] Cragg MS, Kuroda J, Puthalakath H, Huang DCS, and Strasser A (2007). Gefitinib-induced killing of NSCLC cell lines expressing mutant EGFR requires BIM and can be enhanced by BH3 mimetics. *PLoS Med* **4**, 1681–1689; discussion 1690.
- [55] Patel MP, Masood A, Patel PS, and Chanan-Khan AA (2009). Targeting the Bcl-2. *Curr Opin Oncol* **21**, 516–523.
- [56] Oakes SR, Vaillant F, Lim E, Lee L, Breslin K, Feleppa F, Deb S, Ritchie ME, Takano E, Ward T, et al. (2012). Sensitization of BCL-2–expressing breast tumors to chemotherapy by the BH3 mimetic ABT-737. *Proc Natl Acad Sci USA* **109**, 2766–2771.
- [57] Sakakibara-Konishi J, Oizumi S, Kikuchi J, Kikuchi E, Mizugaki H, Kinoshita I, Dosaka-Akita H, and Nishimura M (2012). Expression of bim, noxa, and puma in non-small cell lung cancer. *BMC Cancer* **12**, 286.

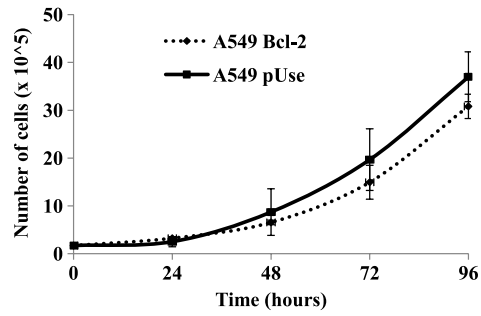


Figure W1. Bcl-2 overexpression does not change doubling time from A549 cell lines. A549 pUse and Bcl-2 cells were incubated at the same concentrations for 24, 48, 72, and 96 hours, and the number of cells was determined for each condition.

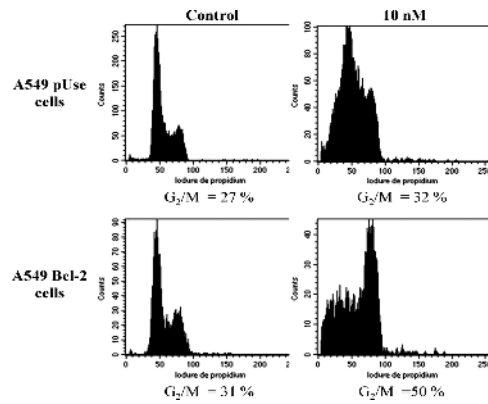


Figure W2. Paclitaxel-mediated G₂/M arrest is enhanced in Bcl-2-overexpressing lung cancer cells. A549 pUse and Bcl-2 cells were incubated with 10 nM paclitaxel for 24 hours. Percentages of G₂/M-arrested cells are indicated. Data represent three independent experiments.

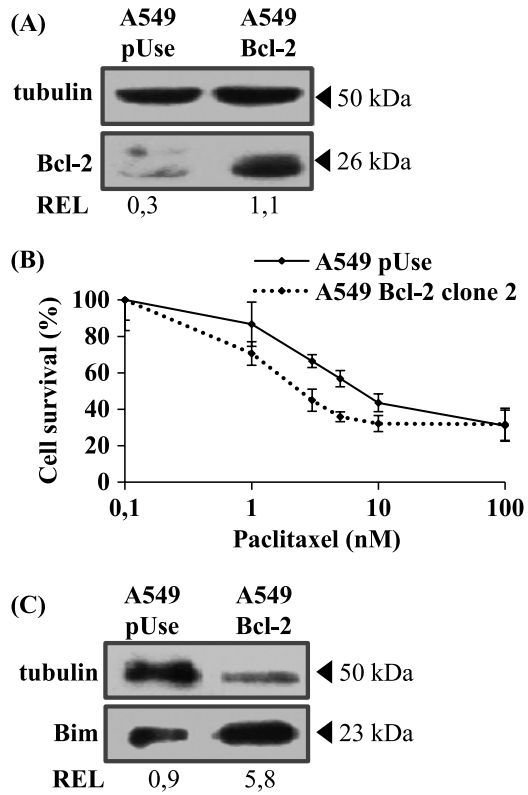


Figure W3. Effect of Bcl-2 overexpression was not clone dependent. (A) Bcl-2 overexpression with no treatment was verified by Western blot analysis on whole-cell lysates of A549 Bcl-2 clone 2. Expression tubulin was used as a loading control to calculate REL. (B) Cytotoxicity of paclitaxel was measured using an MTT assay. (C) Bim overexpression was verified by Western blot analysis on A549 Bcl-2 clone 2 cells.

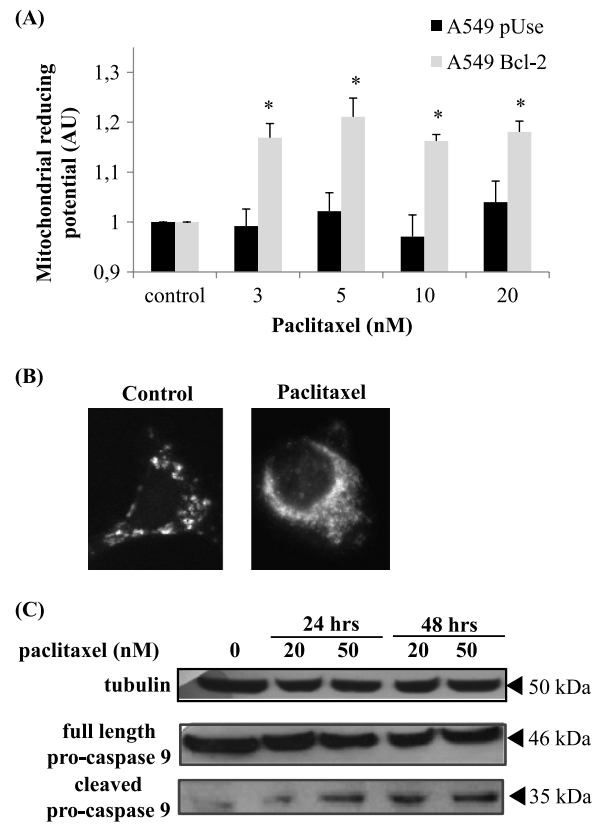


Figure W4. Paclitaxel promptly disturbed mitochondrial functions and permeability in Bcl-2-overexpressed A549 cells. (A) Exponentially growing cells were incubated with a range of paclitaxel concentrations for 6 hours, and mitochondrial reducing potential was assessed using an MTT test (* $P < .05$). (B) Cytochrome *c* localization in the cytosol was viewed by immunofluorescence after paclitaxel treatment. (C) Cleavage of pro-caspase-9 after paclitaxel treatment in A549 Bcl-2 cells.